Generation and measurement of complex laser pulse shapes in the SG-III laser facility

Dongxia Hu (胡东霞), Jun Dong (董 军), Dangpeng Xu (许党朋), Xiaoxia Huang (黄小霞), Wei Zhou (周 伟), Xiaocheng Tian (田小程), Dandan Zhou (周丹丹), Huaiwen Guo (郭怀文), Wei Zhong (钟 伟), Xuewei Deng (邓学伟)*, Qihua Zhu (朱启华), and Wanguo Zheng (郑万国)

Research Center of Laser Fusion, China Academy of Engineering Physics, Mianyang 621900, China

**Corresponding author: xwdeng@caep.cn*

Received December 5, 2014; accepted February 12, 2015; posted online March 13, 2015

The generation and measurement of complex ultraviolet laser pulse shapes is demonstrated in the SG-III laser facility. Relatively high contrast ratio of 300:1 required by the physics experiment is achieved and successfully measured. Two continuous main shots validate the reproduction and the stability of the pulse shape, which provide solid foundation for precise physics experiment and laser power balance.

OCIS codes: 140.3300, 350.2660, 350.4600.

doi: 10.3788/COL201513.041406.

Laser driven inertial confinement fusion (ICF) research requires different types of laser temporal shapes[1–4] and spatial distributions[5]. Some of the temporal shapes are very complicated in order to produce sequential shock waves that compress the target pellet and confine the filled fuel[6]. The precision of these temporal shapes is a key component in meeting the experimental goals so that the technique of generating a precisely shaped laser pulse is always a key issue in the field of high power laser systems for the ICF[7,8]. There have been several huge laser drivers built or under construction around the world, such as the NIF[8] in the U.S., the LMJ[9] in France, and the SG-III laser facility[10] in China. These laser drivers adopted similar techniques in the laser master oscillator room (MOR), also called the front-end system, to generate shaped laser pulses by using an arbitrary waveform generator (AWG). It's reported that, the NIF was capable of producing a shaped ultraviolet laser pulse with a contrast ratio of 150:1 in 2007[8], and this capability was upgraded leading to an increased contrast ratio of 275:1 in 2011[11]. Such a tuning range of laser pulses provides flexibility for different requirements of physics experiments.

The SG-III laser facility is currently the largest laser driver for ICF research in China. It has 48 laser beams and is designed to deliver 180 kJ of ultraviolet laser energy onto the target in 3 ns. The SG-III laser facility is still under construction at present, and is expected to achieve its full output capability at the end of 2015. During its early stage of construction and adjustment, the most used temporal pulse shape is rectangular with a 3 ns pulse duration. With the progress of the construction and the physics experiment, it is more and more urgent to test SG-III's capability of generating complex laser pulse shapes as well as to demonstrate the correctness of the technical pathways of the front-end system. There has been early work in generating shaped laser pulses in previous laser facilities, such as the SG-II laser facility[12,13] and the SG-III prototype[14]. In this Letter, we report the latest pulse shaping experiment results in the SG-III laser facility. The capability of generating and measuring complex pulse shapes demanded by physics experiments is demonstrated. At a limited ultraviolet laser energy level of about 1.9 kJ, the required 300:1 contrast ratio is achieved and successfully measured. By two continuous main shots, the reproduction of the pulse shape is validated, which is very important for providing a stable experiment condition and achieving power balance in the SG-III facility.

The front-end system in the SG-III facility is an all-fiber laser system[15]. A cw laser generated by a distributed feedback (DFB) fiber laser is then modulated to a pulse chain by an electro-optics modulator that is driven by an AWG. One AWG shapes 16 pulse waveforms and, thus in total, three AWGs provide all 48 of the waveforms for the SG-III laser facility. Each of the SG-III's 48 beam lines is capable of generating a unique temporal pulse shape, so it is very convenient to compensate for the laser amplification difference[16] by adjusting the 48 waveforms separately. When generating a shaped laser pulse, for example a 3 ns square pulse, the AWG sums the output of 30 electric impulse generators, each having 150 ps pulse width and 100 ps temporal separation. By adjusting the amplitudes of these 30 electric Gaussian impulse generators to the same level, we can easily get a summation result of a square pulse. Other pulse shapes are generated in the same way by adjusting the impulse generators' amplitudes. Figure 1 shows the schematics of how a shaped laser pulse is generated in the front-end system of the SG-III facility.

The laser pulse shape required by the physics experiment refers to the ultraviolet pulse shape after frequency conversion in the final optics assembly (FOA). Figure 2 explains the whole process for achieving the required laser pulse shape. Once the required ultraviolet pulse shape is set, it is first transferred to a corresponding fundamental pulse

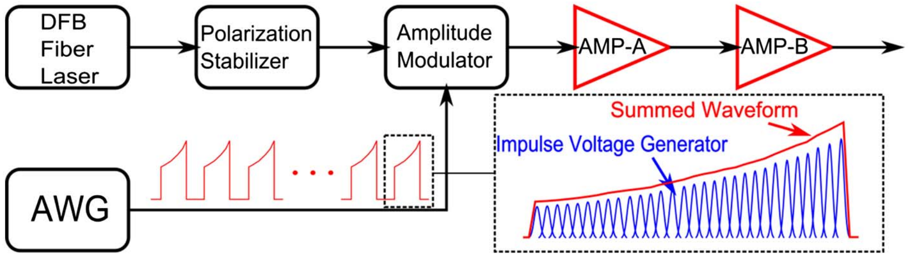

Fig. 1. Schematics of the front-end system of the SG-III facility where the shaped pulse is generated.

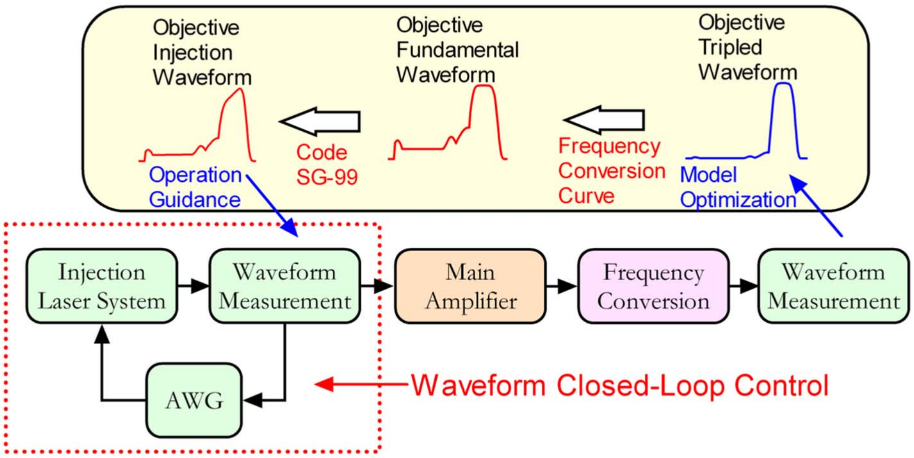

Fig. 2. Whole process of how the SG-III facility achieves the required tripled waveform.

waveform. During this process, the frequency conversion efficiency of a unique beam line is predefined; i.e., the waveform transformation is decided by the frequency conversion curve[17]. Then this fundamental waveform is set as an objective waveform in the model simulation procedure, during which the code SG-99[18] is used and its main parameters have been calibrated by experiments[19]. During this procedure, the objective waveform is initially set as an injected pulse shape, which is then propagated and amplified by the simulation code SG-99. Then we compare the output pulse shape with the objective one, and correspondingly adjust the initial input pulse shape[9]. This iterative shaping process keeps going until a defined convergence criterion has been satisfied. Figure 3(a) gives the objective ultraviolet pulse shape and the corresponding fundamental pulse shape, and Fig. 3(b) shows the simulation result of the required initial input pulse shape. This type of pulse shape is required by the physics experiment, which has a contrast ratio of 300:1. The relatively high contrast ratio has never been demonstrated in previous laser facilities in China. It is a challenge not only for the SG-III facility itself, but also for the pathways for future ICF laser technologies.

Experimentally, one beam line in the SG-III facility is chosen and the beam integrated diagnostic system (BIDS) is used to measure the ultraviolet pulse shape. Figure 4(a) schematically shows the whole experimental setups. A sampling mirror is inserted after the L4 lens and reflects

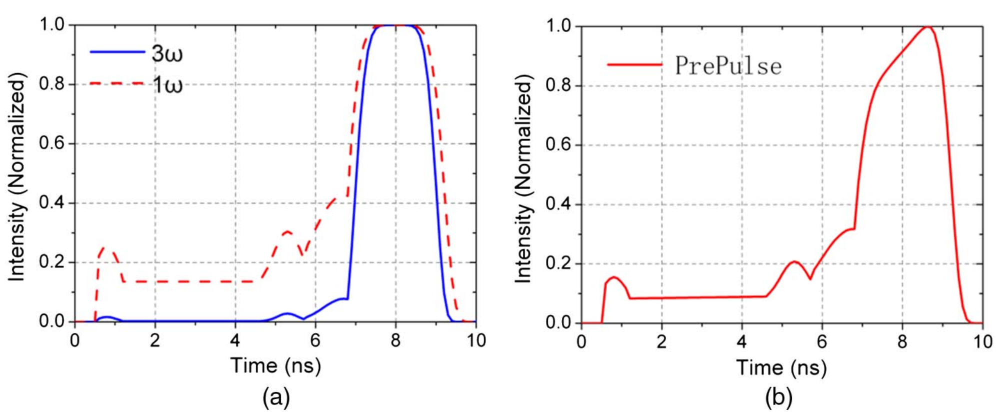

Fig. 3. (a) Objective ultraviolet waveform and the corresponding fundamental waveform; and (b) the simulated initial input waveform in the injection laser system.

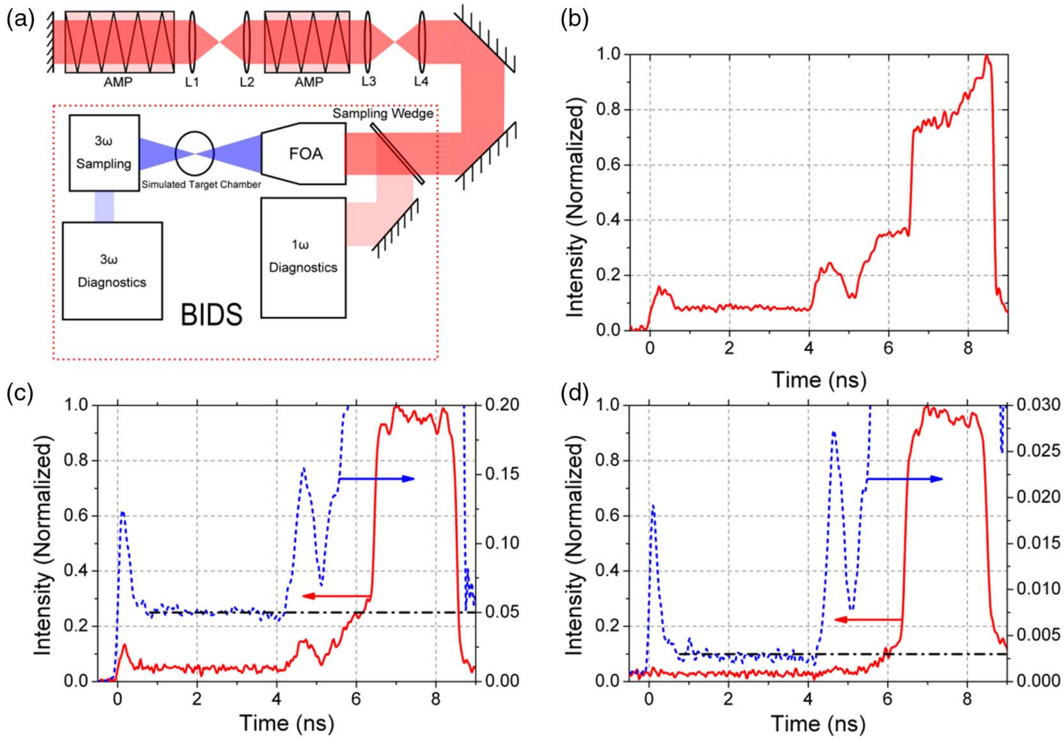

Fig. 4. (a) Schematics of the experimental setups; (b) the pulse shape in the preamplifier; (c) the fundamental and (d) the tripled pulse shapes. The dashed lines show the details of the pulse foots.

the laser to the BIDS instead of the target area. The BIDS contains a FOA that works in the same way as in the target area, and the fundamental and tripled lasers are sampled and measured separately. For a complex laser pulse with a contrast ratio of 300:1, it is hard to clearly measure the foot and the peak sections of the pulse in one signal channel simultaneously. So we divided the pulse shape signal from the photoelectric detector into two channels of the oscilloscope. The first channel is used to measure the whole temporal profile of the pulse, which can clearly exhibit the peak profile. However, the foot of the pulse is too low to be observed in this channel. So the other channel is tuned with a proper attenuation so that the foot section of the pulse can be observed. With this method, both the peak and the foot section of the laser pulse can be measured precisely.

Before the main shot, several preshots were made to ensure the injected energy and the pulse shape. Figure 4(b) shows the laser pulse in the preamplifier system. This shaped pulse was then injected into the main amplifier and amplified to several kJ. This fundamental pulse shape has a relatively low contrast ratio of about 20:1, as shown in Fig. 4(c). The contrast ratio will be magnified during the process of frequency tripling because the foot section experiences a lower frequency conversion efficiency while the peak is higher, which increases the contrast ratio obviously. NIF has reported a 17:1 fundamental contrast ratio that was then magnified to 150:1 after frequency tripling[8]. Figure 4(d) gives the final ultraviolet pulse shape that will actually interact with the target. The result reveals the achieved 300:1 contrast ratio as well as it can be successfully measured. This is the first time we demonstrate that the laser facility is capable of generating an ultraviolet laser with such a relatively high pulse shape contrast ratio of about 300:1. This result also validates the technical pathways of our front-end system in high power laser facilities. In fact, we have further tested the capability of generating and measuring a complex laser pulse shape with a contrast ratio as high as 1000:1 at the same energy level in the subsequent experiments. Although the contrast ratio will decrease with energy increasing, due to the saturation effect, the experiment results still give us confidence that our front-end system can provide flexible tuning capability and the diagnostics system can clearly resolve the detailed pulse shape.

For routine operation, the facility must provide stable laser performance. So 4 h after the first main shot as shown in Fig. 4, the other main shot was made to validate the reproduction of the laser pulse shape. During these 4 h, no change was made to the laser facility. So the laser pulse we used is the same one as in Fig. 4, whose pulse duration is 9 ns. The result compared with the first main shot is shown in Fig. 5. The ultraviolet laser energy is 1903 J compared with 1913 J of the first shot, only 0.5% deviation. In the second main shot, the foot remains 1/300 the maximum of the peak, and the prepulse, the foot section, and the second pulse are near copies from those of the first shot. There is only a little difference in the peak of the laser pulse shape. This difference is most probably induced by the fluctuation of the front-end system, which leads to the FM-to-AM effect when the laser pulse propagates from the optics fiber system to the preamplifier system[20]. Actually, a

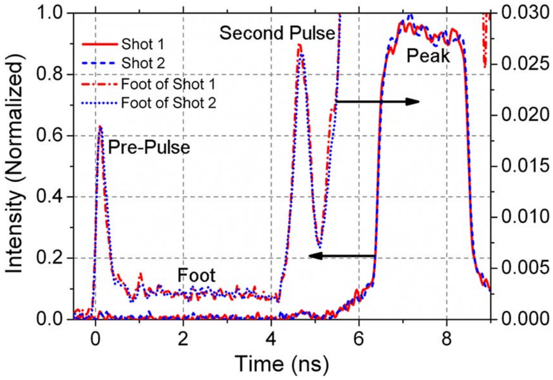

Fig. 5. Waveform comparison between the two main shots. The solid lines give the whole waveforms, while the dashed lines give the details of the foot.

closed-loop control technique has been planned to suppress the FM-to-AM effect automatically in the SG-III performance upgrade project. The pulse peak power in the experiment is about 0.9 TW, still below the designed maximum operation point of 1.25 TW per beam, while the experiment result reveals a good reproduction of the laser pulse shape and the energy. It is a solid foundation to provide a stable experimental condition and achieve laser power balance[21,22].

In conclusion, we demonstrate the SG-III's capability of experimentally generating and measuring complex laser pulse shapes with a relatively high contrast ratio. With the calibrated simulation code SG-99 and the proper closed loop pulse shape adjustment in the front end system, a complex ultraviolet laser pulse shape with a contrast ratio of 300:1 is successfully generated, which meets well the requirements of the physics experiment. A two-channel multiplexing measurement method is used to obtain the pulse details of the foot and peak sections separately. The experimental results also validate the technical pathways of the front-end system for future high power laser facilities. With two continuous main shots, we reveal the facility's stability in output energy and laser pulse shape, which provide a solid foundation for a precise physics experiment and laser power balance.

The authors thank all the colleagues in the Laser Engineering Division of the Research Center of Laser Fusion who were not listed as co-authors, but have made great contributions to this work.

References

1. R. Betti, C. D. Zhou, K. S. Anderson, L. J. Perkins, W. Theobald, and A. A. Solodov, Phys. Rev. Lett. **98**, 155001 (2007).
2. O. A. Hurricane, D. A. Callahan, D. T. Casey, P. M. Celliers, C. Cerjan, E. L. Dewald, T. R. Dittrich, T. Doppner, D. E. Hinkel, L. F. B. Hopkins, J. L. Kline, S. Le Pape, T. Ma, A. G. MacPhee, J. L. Milovich, A. Pak, H. S. Park, P. K. Patel, B. A. Remington, J. D. Salmonson, P. T. Springer, and R. Tommasini, Nature **506**, 343 (2014).
3. O. A. Hurricane, D. A. Callahan, D. T. Casey, E. L. Dewald, T. R. Dittrich, T. Döppner, M. A. Barrios Garcia, D. E. Hinkel, L. F. Berzak Hopkins, P. Kervin, J. L. Kline, S. L. Pape, T. Ma, A. G. MacPhee, J. L. Milovich, J. Moody, A. E. Pak, P. K. Patel, H.-S. Park, B. A. Remington, H. F. Robey, J. D. Salmonson, P. T. Springer, R. Tommasini, L. R. Benedetti, J. A. Caggiano, P. Celliers, C. Cerjan, R. Dylla-Spears, D. Edgell, M. J. Edwards, D. Fittinghoff, G. P. Grim, N. Guler, N. Izumi, J. A. Frenje, M. Gatu Johnson, S. Haan, R. Hatarik, H. Herrmann, S. Khan, J. Knauer, B. J. Kozioziemski, A. L. Kritcher, G. Kyrala, S. A. Maclaren, F. E. Merrill, P. Michel, J. Ralph, J. S. Ross, J. R. Rygg, M. B. Schneider, B. K. Spears, K. Widmann, and C. B. Yeamans, Phys. Plasmas **21**, 056314 (2014).
4. J. D. Lindl, P. Amendt, R. L. Berger, S. G. Glendinning, S. H. Glenzer, S. W. Haan, R. L. Kauffman, O. L. Landen, and L. J. Suter, Phys. Plasmas **11**, 339 (2004).
5. Y. Jiang, S. Zhou, R. Wu, J. Li, X. Li, and Z. Lin, Chin. Opt. Lett. **11**, 081404 (2013).
6. H.-B. Cai, S.-Z. Wu, J.-F. Wu, M. Chen, H. Zhang, M.-Q. He, L.-H. Cao, C.-T. Zhou, S.-P. Zhu, and X.-T. He, High Power Laser Sci. Eng. **2**, e6 (2014).
7. P. J. Wisoff, M. W. Bowers, G. V. Erbert, D. F. Browning, and D. R. Jedlovec, Proc. SPIE **5341**, 146 (2004).
8. C. A. Haynam, P. J. Wegner, J. M. Auerbach, M. W. Bowers, S. N. Dixit, G. V. Erbert, G. M. Heestand, M. A. Henesian, M. R. Hermann, K. S. Jancaitis, K. R. Manes, C. D. Marshall, N. C. Mehta, J. Menapace, E. Moses, J. R. Murray, M. C. Nostrand, C. D. Orth, R. Patterson, R. A. Sacks, M. J. Shaw, M. Spaeth, S. B. Sutton, W. H. Williams, C. C. Widmayer, R. K. White, S. T. Yang, and B. M. Van Wonterghem, Appl. Opt. **46**, 3276 (2007).
9. B. J. L. Garrec and O. Nicolas, J. Phys. **112**, 032019 (2008).
10. W. Zheng, X. Zhang, X. Wei, F. Jing, Z. Sui, K. Zheng, X. Yuan, X. Jiang, J. Su, H. Zhou, M. Li, J. Wang, D. Hu, S. He, Y. Xiang, Z. Peng, B. Feng, L. Guo, X. Li, Q. Zhu, H. Yu, Y. You, D. Fan, and W. Zhang, J. Phys. **112**, 032009 (2008).
11. G. Brunton, G. Erbert, D. Browning, and E. Tse, Fusion Eng. Des. **87**, 1940 (2012).
12. C. Wang, S. H. Chen, F. M. Xu, X. L. Xie, X. P. Ge, S. H. Xu, Z. Q. Lin, D. Y. Fan, and X. M. Deng, Chin. J. Quantum Electron. **17**, 479 (2000).
13. S. Yi, B. Mu, J. Zhu, X. Wang, W. Li, Z. Wang, P. He, W. Wang, Z. Fang, and S. Fu, Chin. Opt. Lett. **12**, 083401 (2014).
14. W. Wang, R. Zhao, J. Su, H. Li, Y. Liang, L. Mo, F. Wang, L. Liu, Z. Sun, Q. Zhu, and A. Jing, Acta Opt. Sin. **30**, 1051 (2010).
15. R. Zhang, J. Wang, H. Lin, M. Li, Y. Che, Z. Lu, and Y. Deng, Chin. J. Lasers **36**, 160 (2009).
16. P. Li, F. Jing, D. Wu, R. Zhao, H. Li, H. Lin, and J. Su, Proc. SPIE **8433**, 843317 (2012).
17. P. J. Wegner, J. M. Auerbach, J. T. A. Biesiada, S. N. Dixit, J. K. Lawson, J. A. Menapace, T. G. Parham, D. W. Swift, P. K. Whitman, and W. H. Williams, Proc. SPIE **5341**, 180 (2004).
18. W. Deng, K. Zhang, X. Jiang, W. Dai, W. Zhou, X. Zhang, J. Zhao, and D. Hu, High Power Laser Part. Beams **23**, 2608 (2011).
19. M. Shaw, R. House, W. Williams, C. Haynam, R. White, C. Orth, and R. Sacks, J. Phys. **112**, 032022 (2008).
20. D. Xu, J. Wang, M. Li, H. Lin, R. Zhang, Y. Deng, Q. Deng, X. Huang, M. Wang, L. Ding, and J. Tang, Opt. Express **18**, 6621 (2010).
21. S. Glenzer, O. S. Jones, D. R. Speck, D. Munro, R. Lerche, T. Salmon, E. Bliss, A. Gates, B. Boyd, J. Auerbach, W. Williams, A. Saroyan, D. Kalantar, B. MacGowan, R. Zacharias, C. Haynam, and R. Sacks, "3ω power balance procedure on the NIF," UCRL-ID-142777 (2001).
22. G. A. Kyrala, A. Seifter, J. L. Kline, S. R. Goldman, S. H. Batha, and N. M. Hoffman, Phys. Plasmas **18**, 072703 (2011).